Simultaneous measurement of refractive index and temperature using a microring resonator

Nai Lin (林 奈), Lan Jiang (姜 澜)*, Sumei Wang (王素梅), Lei Yuan (袁 雷), and Qianghua Chen (陈强华)

Laser Micro/Nano Fabrication Laboratory, School of Mechanical Engineering, Beijing Institute of Technology, Beijing 100081, China

**Corresponding author: jianglan@bit.edu.cn*

Received October 11, 2011; accepted December 12, 2011; posted online February 24, 2012

An approach to the simultaneous measurement of refractive-index (RI) and temperature changes using optical ring resonators is proposed and theoretically demonstrated. With a liquid-core silica ring resonator as an example, two different-order whispering gallery modes (WGMs) might differ in not only RI but also temperature sensitivities. Thus, a second-order sensing matrix should be defined based on these WGMs to determine RI and temperature changes simultaneously. The analysis shows that the RI and temperature detection limits can be achieved on the order of 10^{-7} RI unit and 10^{-3} K at a wavelength of approximately 780 nm.

OCIS codes: 280.4788, 280.6780, 140.4780.
doi: 10.3788/COL201210.052802.

Optical microresonators of various shapes, such as microdisks[1], microtoroids[2,3], microspheres[4,5], and microrings[6−10], have been widely studied. In these resonators, light propagates in the form of whispering gallery modes (WGMs) because of its total internal reflection along the curved boundary between high and low refractive-index (RI) materials. Microresonators with WGMs are widely used as RI sensors for biological material detection[4,9] and chemical-concentration-change measurements[5−8], among others, because of the high Q factors and, thus, long light-material interaction paths. However, WGMs are also sensitive to thermal fluctuations induced by environmental temperature variations or probe-induced energy absorptions. In particular, for RI sensors with high Q factors, the resonance instability due to temperature-induced fluctuations significantly impairs sensor performance[11]. In such cases, temperature control devices, such as thermoelectric cooling units, are usually implemented to ensure small temperature fluctuations[12]. Another way of reducing resonance thermal drift is the introduction of some materials with negative thermal-optic coefficients in the cavity mode volume to compensate the positive thermal-optic coefficient of the ring resonator material[13−15]. However, this method requires precise control of the coating layer thickness[13,14] or resonator size[15]. In practice, achieving such precision, where the thermal drift can be eliminated, is difficult. Moreover, some nonuniformity of the coating layer or resonator further increases residual thermal drift. Meanwhile, the ultrasensitive shift of the WGM resonance to the ambient temperature can be used to design highly sensitive thermal sensors[16−18], for which the bulk RI should be kept unchanged.

This letter theoretically analyzes the use of optical ring resonators for the simultaneous measurement of RI and temperature changes. Both the RI and temperature sensitivities of the WGMs in a ring resonator are studied as a function of the ring wall thickness and WGM order. The results show that a ring resonator of any wall thickness has two WGMs of different orders with different RI and temperature sensitivities. By monitoring the resonant wavelength shifts of the WGMs of these two orders, a second-order sensing matrix can be defined to determine the RI and temperature changes simultaneously. A prism coupler[8] or a fused-tapered fiber tip[19] can be used to excite WGMs of several different orders selectively and efficiently within the same wavelength range, providing the basis for the implementation of the proposed approach. The most important contribution of the proposed scheme is its ability to eliminate the thermal noise induced by the environment temperature fluctuation or the probe-light-induced cavity temperature variation, considering that it detects both temperature and RI changes.

For a ring resonator, the WGM can be characterized by a set of integers, namely, m and v, which represent the angular and radial (also known as the WGM order) mode numbers, respectively. In addition, the WGM has two polarizations, namely, the transverse electric (TE) and magnetic (TM) modes, with the magnetic and electric fields along the cylinder longitudinal direction, respectively. The two polarizations can be selectively excited by controlling the polarization of the coupling light, and the WGM responses to the RI and temperature changes are slightly varied with the mode polarizations[20]. For simplicity and without losing the generality of the discussion, this study considers TM modes only. Taking a ring resonator with inner and outer radii (R_1 and R_2, respectively) as an example (shown in the inset of Fig. 1), the characteristic equation for specifying the resonant wavelength $\lambda_{\rm R}$ of the TM modes can be expressed as[21]

$$\frac{n_3}{n_2}\frac{H_m'^{(1)}(\overrightarrow{k}_0 n_3 R_2)}{H_m^{(1)}(\overrightarrow{k}_0 n_3 R_2)} = \frac{B_m J_m'(\overrightarrow{k}_0 n_2 R_2) + H_m'^{(1)}(\overrightarrow{k}_0 n_2 R_2)}{B_m J_m(\overrightarrow{k}_0 n_2 R_2) + H_m^{(1)}(\overrightarrow{k}_0 n_2 R_2)}, \tag{1}$$

$$B_m = \frac{n_2 J_m(\overrightarrow{k}_0 n_1 R_1) H_m'^{(1)}(\overrightarrow{k}_0 n_2 R_1) - n_1 J_m'(\overrightarrow{k}_0 n_1 R_1) H_m^{(1)}(\overrightarrow{k}_0 n_2 R_1)}{n_1 J_m'(\overrightarrow{k}_0 n_1 R_1) J_m(\overrightarrow{k}_0 n_2 R_1) - n_2 J_m(\overrightarrow{k}_0 n_1 R_1) J_m'(\overrightarrow{k}_0 n_2 R_1)}, \tag{2}$$

where $\overrightarrow{k}_0 = 2\pi/\lambda_{\rm R}$ is the resonant wave vector, and n_1, n_2, and n_3 are the RIs of the ring core, ring wall, and surrounding medium, respectively. In Eqs. (1) and (2), J_m and $H_m^{(1)}$ are the mth Bessel and Hankel functions of the first kind, respectively. For a given value of m, multiple values of $\lambda_{\rm R}$ satisfy the characteristic equation. These resonant modes are called the first-order mode, the second-order mode, $\cdots$, and the vth-order mode, and so on as the $\lambda_{\rm R}$ value decreases.

Considering a uniform RI change (δn_1) in the ring core, a shift $\delta\lambda_{\rm R}$ in the resonant wavelength would occur correspondingly according to the characteristic equation. Moreover, a temperature change δT would result in the resonant wavelength shift through the thermal expansion and thermo-optic effects[13]. The RI ($S_{\rm RI}$) and temperature ($S_{\rm T}$) sensitivities, defined as the resonant wavelength shift versus the RI and temperature changes, respectively, can be expressed as[20]

$$S_{\rm RI} = \frac{\delta\lambda_{\rm R}}{\delta n_1} \approx \frac{\lambda_{\rm R}}{n_1}\eta_1, \tag{3}$$

$$S_{\rm T} = \frac{\delta\lambda_{\rm R}}{\delta T} \approx \lambda_{\rm R}\left[\frac{\sum\limits_{i=1}^{3}\eta_i({\rm d}n_i/{\rm d}T)}{\sum\limits_{i=1}^{3}\eta_i n_i} + \alpha\right], \tag{4}$$

where η_1, η_2, and η_3 denote the fractions of light energy distributed in the ring core, ring wall, and surrounding medium, respectively, ${\rm d}n_i/{\rm d}T$ is the thermal refraction coefficient of the corresponding material, and α is the linear thermal expansion coefficient of the whole ring resonator. The energy fractions can be calculated as

$$\eta_i = \frac{n_i^2\int_{V_i}|T(r)|^2\,{\rm d}r}{\int_V n^2|T(r)|^2\,{\rm d}r},\ i=1,2,3, \tag{5}$$

where V denotes the entire space and $T(r)$ is the function for describing the electric field distribution of the WGMs along the radial direction, which is given as

$$T(r)=\begin{cases} A_m J_m(\overrightarrow{k}_0 n_1 r) & V_1: r<R_1 \\ B_m J_m(\overrightarrow{k}_0 n_2 r)+H_m^{(1)}(\overrightarrow{k}_0 n_2 r) & V_2: R_1<r<R_2, \\ C_m H_m^{(1)}(\overrightarrow{k}_0 n_3 r) & V_3: r>R_2 \end{cases} \tag{6}$$

$$\begin{cases} A_m = \dfrac{B_m J_m(\overrightarrow{k}_0 n_2 R_1)+H_m^{(1)}(\overrightarrow{k}_0 n_2 R_1)}{J_m(\overrightarrow{k}_0 n_1 R_1)} \\ C_m = \dfrac{B_m J_m(\overrightarrow{k}_0 n_2 R_2)+H_m^{(1)}(\overrightarrow{k}_0 n_2 R_2)}{H_m^{(1)}(\overrightarrow{k}_0 n_3 R_2)} \end{cases}, \tag{7}$$

According to Eqs. (3) and (4), the RI and temperature sensitivities are both functions of the energy fractions, which might be different for WGMs of different orders. We consider a liquid-core silica ring resonator (LCSRR) as an example[6−10]. The RIs are chosen as $n_1 = 1.33$ for the liquid core (primarily composed of water), $n_2 = 1.45$ for the silica ring wall, and $n_3 = 1.0$ for the air surrounding the ring resonator. The thermal refraction coefficients of water, silica, and air are approximately -10^{-4}, 6.4×10^{-6}, and 10^{-6}/K, respectively, and the linear thermal expansion coefficient of the liquid-core silica resonator is approximately 5.0×10^{-7}/K[15]. The thickness of the silica ring wall is denoted as h (i.e., $h = R_2 - R_1$). Figure 1 shows the normalized electric field intensity distributions for the TM modes of the first two orders at $\lambda_{\rm R}\approx780$ nm in a LCSRR of $R_2 = 50$ μm and $h = 1.5$ μm. Angular mode numbers of $m = 569$ for $v = 1$ and $m = 550$ for $v = 2$ are selected to keep the resonance at approximately 780 nm. As shown in Fig. 1, the energy fractions in the liquid core are $\eta_1 = 0.5\%$ and 5% for the first- and second-order TM modes, which correspond to RI sensitivities of ∼2.9 and ∼29 nm/RIU (RIU: RI unit), respectively, according to Eq. (3). In addition, the temperature sensitivities of the first- and second-order TM modes are calculated as 3.5 and 1.0 pm/K, respectively, after substituting the energy fractions into Eq. (4). Thus, the following character matrix $\mathbf{M}_{\rm RI,T}$ can be defined to represent the sensing performance of the WGMs of the first-two orders:

$$\begin{aligned}\begin{bmatrix}(\delta\lambda_{\rm R})_{v=1}\\(\delta\lambda_{\rm R})_{v=2}\end{bmatrix} &= \mathbf{M}_{\rm RI,T}\begin{bmatrix}\delta n_1\\ \delta T\end{bmatrix} \\ &= \begin{bmatrix}(S_{\rm RI})_{v=1} & (S_{\rm T})_{v=1}\\(S_{\rm RI})_{v=2} & (S_{\rm T})_{v=2}\end{bmatrix}\begin{bmatrix}\delta n_1\\ \delta T\end{bmatrix},\end{aligned} \tag{8}$$

where the subscript v= 1, 2 identifies the resonant wavelength shift and sensitivity for the WGM of the corresponding order. Then, the RI and temperature changes can be simultaneously determined by monitoring the resonance shifts of the WGMs of the first two orders as

$$\begin{aligned}\begin{bmatrix}\delta n_1\\ \delta T\end{bmatrix} &= M_{\rm RI,T}^{-1}\begin{bmatrix}(\delta\lambda_{\rm R})_{v=1}\\(\delta\lambda_{\rm R})_{v=2}\end{bmatrix} \\ &= \begin{bmatrix}-0.01 & 0.04\\ 0.29 & -0.03\end{bmatrix}\begin{bmatrix}(\delta\lambda_{\rm R})_{v=1}\\(\delta\lambda_{\rm R})_{v=2}\end{bmatrix}.\end{aligned} \tag{9}$$

The RI and temperature detection limits, defined as the smallest detectable RI and temperature changes, respectively, can be estimated by substituting the wavelength resolution $(\delta\lambda_{\rm R})_{\rm min}$ into the two-dimensional sensing equations. In previously reported RI sensing applications using optical microresonators, the wavelength resolution is determined by two factors: the thermal noise

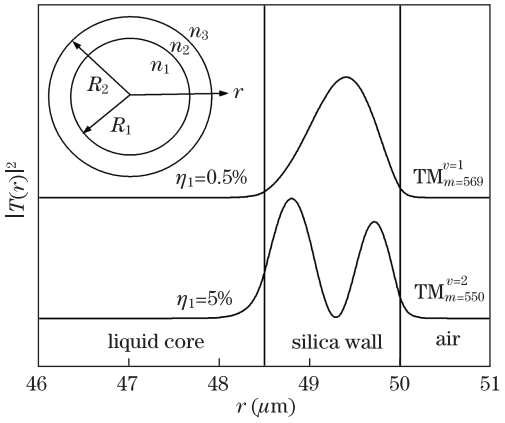

Fig. 1. Normalized electric field intensity distributions for the TM modes of the first two orders of a ring resonator of $h = 1.5$ μm at $\lambda_{\rm R}\approx780$ nm. (Inset: schematic structure of a ring resonator).

and WGM resonance linewidth[11,12]. In this letter, the proposed mechanism determines the temperature change simultaneously with the RI change. Therefore, the temperature variation is no longer considered noise. The resonance linewidth $\Delta\lambda_R$ is further related to the Q factor as $\Delta\lambda_R = \lambda_R/Q$. The Q factor of the LCSRR is determined by the lumped loss of light in the resonator, which includes the radiation loss (also known as tunneling loss), the scattering loss from surface irregularities, and the material absorption loss of light. Considering a LCSRR of $R_2 = 50$ μm and $h = 1.5$ μm, the fields of the first two-order WGMs at $\lambda_R \approx 780$ nm are tightly confined in the silica wall region, as shown in Fig. 1, leading to a very low radiation loss. The material absorption loss of light in the visible band is also very low, and thus, the total Q factor is mainly limited by the scattering loss[8]. The high temperature used in fabricating the LCSRR ensures a very smooth surface, and Q factors approaching 10^6 have been reported[22]. As for such high Q factors, the wavelength resolution without thermal noise can easily be a few tens of femtometers[11,12]. Therefore, based on Eq. (9), the RI and temperature detection limits can be expected to be on the order of 10^{-7} RIU and 10^{-3} K, respectively.

Figure 2 shows the S_{RI} and S_T values for the TM modes of the first three orders in a LCSRR of $h = 0$ to 3 μm at $\lambda_R \approx 780$ nm. The outer radius of the ring resonator is kept at $R_2 = 50$ μm for all cases. The negative sign of S_T indicates that the resonant wavelength decreases as temperature increases. When h increases, the light energy in the liquid core is gradually transferred into the silica wall (i.e., η_1 decreases while η_2 increases), leading to a reduction in S_{RI}, as shown in Fig. 2. Moreover, as a result, the positive thermal refraction of the silica wall becomes dominant and compensates the negative thermal refraction of the liquid core, finally leading to the change in S_T from negative to positive. From Fig. 2, for a thin-walled LCSRR, the modes of not only the first two but also the first three orders might have different RI and temperature sensitivities. For instance, at $h = 1.5$ μm, the sensing matrix can also be established based on the second- and third-order modes because of their different responses to RI and temperature changes, as shown in the insets of Fig. 2. The S_{RI} (or S_T) change of a higher order mode takes an oscillatory path because the light energy from the silica wall to the liquid core decreases as h increases. In other words, modes of different higher orders might have the same light energy distributions and, thus, the same RI and temperature sensitivities at some specific values of h. Figure 2 shows that, at $h \approx 0.5$ μm, the S_{RI} and S_T values of the third-order TM mode are equal to those of the second-order TM mode. Moreover, the sensing matrix cannot be established based on the TM modes of these two orders only.

For the modes of the first three orders at $h >\sim 3$ μm, the light energy is almost completely distributed inside the ring wall (i.e., $\eta_1 = 0$ and $\eta_2 =\sim 1$) and thus corresponds to an S_{RI}, as well as S_T, of zero. However, a thick-walled LCSRR has two different-order modes with different RI and temperature sensitivities. These two modes can be utilized to establish the sensing matrix. Considering the TM modes of three much higher orders ($v = 35$, 36, and 37) in a LCSRR of $R_2 = 166$ μm and

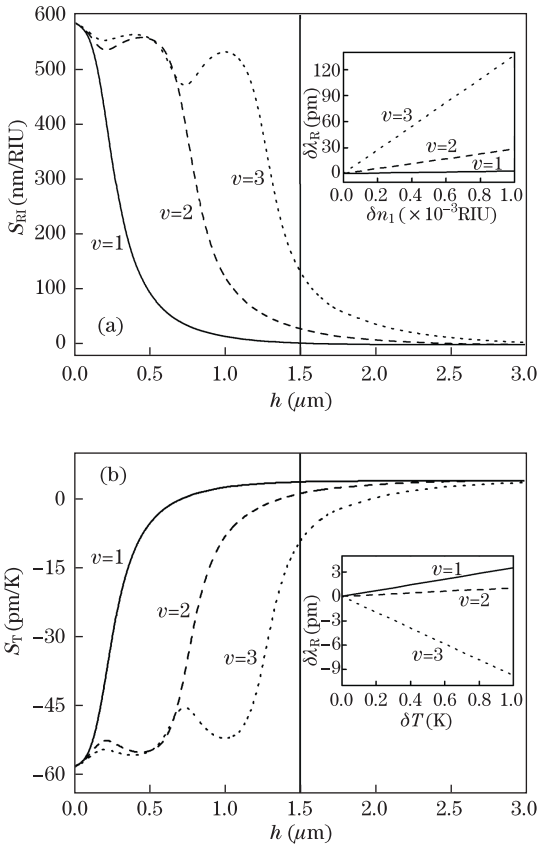

Fig. 2. (a) S_{RI} and (b) S_T as a function of the ring wall thickness h for the TM modes of the first (solid curves), the second (dashed curves), and the third (dotted curves) orders, respectively, at $\lambda_R \approx 780$ nm. (Inset: $\delta\lambda_R$ as a function of (a) δn_1 and (b) δT at $h = 1.5$ μm, in which the slopes of the lines denote the sensitivities).

$h = 32$ μm[8], the S_{RI} and S_T values of $v = 37$ are much larger than those of $v = 35$ or 36 at $\lambda_R \approx 1\,550$ nm, as shown in Table 1. Angular mode numbers of m= 714, 707, and 700 were selected for $v = 35$ to 37, respectively, to keep λ_R at approximately 1 550 nm. Hence, for such a thick-walled ring resonator, the sensing matrix $\mathbf{M}_{RI,T}$ can be established based on the TM modes of any two orders of $v = 35$ to 37. As an example, the RI and temperature variations can be simultaneously determined as follows by monitoring the resonance shifts of the TM modes of $v = 35$ and 37:

$$\begin{bmatrix} \delta n_1 \\ \delta T \end{bmatrix} = \begin{bmatrix} 1.3\times10^{-2} & 3.5\times10^{-4} \\ 1.4\times10^{-1} & -1.4\times10^{-2} \end{bmatrix} \begin{bmatrix} (\delta\lambda_R)_{v=35} \\ (\delta\lambda_R)_{v=37} \end{bmatrix}. \quad (10)$$

Table 1. Sensitivities and Q Factors for TM Modes of $v = 35$ to 37 at $\lambda_R \approx 1\,550$ nm in a Thick-Walled LCSRR

	$TM_{m=714}^{v=35}$	$TM_{m=707}^{v=36}$	$TM_{m=700}^{v=37}$
η_1	5.2%	12.6%	54.1%
S_{RI} (nm/RIU)	61.6	147.9	636.1
S_T (pm/K)	1.6	−6.9	−56.9
Q	4.6×10^4	1.9×10^4	0.4×10^4

If the working wavelength of the LCSRR-based sensor is in the near-infrared band, the Q factor is mainly limited by the large absorption loss of light in water[8]. Moreover, the absorption-loss-limited Q factor can be given as $Q = 2\pi n_1/(\lambda_{\rm R}\alpha_1\eta_1)$[20], where α_1 is the optical attenuation coefficient of water ($\alpha_1 = 2.2 \times 10^3$ m^{-1} at $\lambda_{\rm R} \approx 1\,550$ nm[23]). Considering a LCSRR of $R_2 = 166$ μm and $h = 32$ μm, the water absorption loss results in a low Q factor on the order of 10^4 for the TM modes of $v = 35$ to 37 at $\lambda_{\rm R} \approx 1\,550$ nm, as listed in Table 1. For a detection system with a resolution of 1/25 of the resonance linewidth[8], the wavelength resolutions are approximately $(\delta\lambda_{\rm R})_{\rm min} = 1.3$ and 13.8 pm for the TM modes of $v = 35$ and 37, respectively. Therefore, based on Eq. (10), the RI and temperature detection limits are estimated to be approximately 2.2×10^{-5} RIU and 5.6×10^{-3} K, respectively.

In conclusion, an approach to the simultaneous measurement of RI and temperature changes using WGMs in an optical ring resonator is theoretically demonstrated. Compared with the sensing mechanisms of ring resonators reported so far, the proposed approach allows the ring-resonator-based sensors to work in an environment where both the RI and temperature change significantly. Although only the bulk index sensing is considered in this letter, the proposed approach can also be applied to surface sensing, because surface sensitivity linearly depends on bulk RI sensitivity[9]. In addition, the WGM responses of a surface-layer-coated microsphere resonator to RI and temperature changes also vary with the WGM orders[24]. This finding can also be a basis for the simultaneous measurement of RI and temperature changes. Another exciting research direction is the simultaneous measurement of more variables (such as force, pressure, and acceleration) by defining a higher order sensing matrix.

This work was supported by the National "973" Program of China (No. 2011CB013000) and the National Natural Science Foundation of China (Nos. 90923039 and 51025521).

References

1. E. Krioukov, D. J. W. Klunder, A. Driessen, J. Greve, and C. Otto, Opt. Lett. **27,** 512 (2002).
2. T. J. Kippenberg, S. M. Spillane, D. K. Armani, and K. J. Vahala, Opt. Lett. **29,** 1224 (2004).
3. X. Wu, C. Zou, W. Wei, F. Sun, G. Guo, and Z. Han, Chin. Opt. Lett. **8,** 709 (2010).
4. S. Arnold, M. Khoshsima, I. Teraoka, S. Holler, and F. Vollmer, Opt. Lett. **28,** 272 (2003).
5. N. M. Hanumegowda, C. J. Stica, B. C. Patel, I. M. White, and X. Fan, Appl. Phys. Lett. **87,** 201107 (2005).
6. I. M. White, H. Oveys, and X. Fan, Opt. Lett. **31,** 1319 (2006).
7. V. Zamora, A. Díez, M. V. Andrés, and B. Gimeno, Opt. Express **15,** 12011 (2007).
8. T. Ling and L. J. Guo, Opt. Express **15,** 17424 (2007).
9. H. Zhu, I. M. White, J. D. Suter, P. S. Dale, and X. Fan, Opt. Express **15,** 9139 (2007).
10. V. Zamora, A. Díez, M. V. Andrés, and B. Gimeno, Photon. Nano. Fund. Appl. **9,** 149 (2011).
11. I. M. White and X. D. Fan, Opt. Express **16,** 1020 (2008).
12. X. D. Fan, I. M. White, H. Zhu, J. D. Suter, and H. Oveys, Proc. SPIE **6452,** 6452M (2007).
13. M. Han and A. Wang, Opt. Lett. **32,** 1800 (2007).
14. L. He, Y. F. Xiao, C. Dong, J. Zhu, V. Gaddam, and L. Yang, Appl. Phys. Lett. **93,** 201102 (2008).
15. J. D. Suter, I. M. White, H. Zhu, and X. Fan, Appl. Opt. **46,** 389 (2007).
16. Q. L. Ma, T. Rossmann, and Z. X. Guo, J. Phys. D Appl. Phys. **41,** 245111 (2008).
17. C. H. Dong, L. He, Y. F. Xiao, V. R. Gaddam, S. K. Ozdemir, Z. F. Han, G. C. Guo, and L. Yang, Appl. Phys. Lett. **94,** 231119 (2009).
18. B. B. Li, Q. Y. Wang, Y. F. Xiao, X. F. Jiang, Y. Li, L. X. Xiao, and Q. H. Gong, Appl. Phys. Lett. **96,** 251109 (2010).
19. L. Arques, A. Carrascosa, V. Zamora, A. Díez, J. L. Cruz, and M. V. Andrés, Opt. Lett. **36,** 3452 (2011).
20. N. Lin, L. Jiang, S. M. Wang, H. Xiao, Y. F. Lu, and H. L. Tsai, Appl. Opt. **50,** 3615 (2011).
21. T. Ling and L. J. Guo, J. Opt. Soc. Am. B **26,** 471 (2009).
22. I. M. White, J. D. Suter, H. Oveys, and X. D. Fan, Opt. Express **15,** 646 (2007).
23. G. M. Hale and M. R. Querry, Appl. Opt. **12,** 555 (1973).
24. N. Lin, L. Jiang, S. M. Wang, H. Xiao, Y. F. Lu, and H. L. Tsai, Appl. Opt. **50,** 992 (2011).